# Complications in Correlating Thermal Inertia and Olivine Abundance on Mars

R.D. Hanna[1] and V.E. Hamilton[2]

[1]Jackson School of Geological Sciences, University of Texas, Austin, TX 78712 (romy@jsg.utexas.edu) [2]Southwest Research Institute, Boulder, CO 80302 (hamilton@boulder.swri.edu)

## INTRODUCTION

- Chemical weathering of bedrock to sediment can modify mineralogy.
- Mars's surface is dominated by sediment [1] but this may not represent an unmodified primary igneous lithology [e.g. 2, 3].
- Secondary phases (phyllosilicates, hydrated sulfates, silica) detected (CRISM, MER) but limited and localized [e.g. 4-7].
- Olivine is sensitive to chemical weathering and may be preferentially removed as rock is weathered to sediment [e.g. 8-10].
- Localized studies on Mars suggest that chemical weathering of olivine is creating relatively olivine-poor sediment and it is hypothesized that this may be operating on a global scale [11,12].
- *If chemical weathering dominates Martian sediment production [11,12], sediments derived from olivine-rich bedrock should have a lower olivine content than the bedrock from which they originated.*
- Thermal inertia can be used as a proxy for mean particle size; relatively higher thermal inertias are rockier and lower thermal inertia surfaces are dominated by sands.

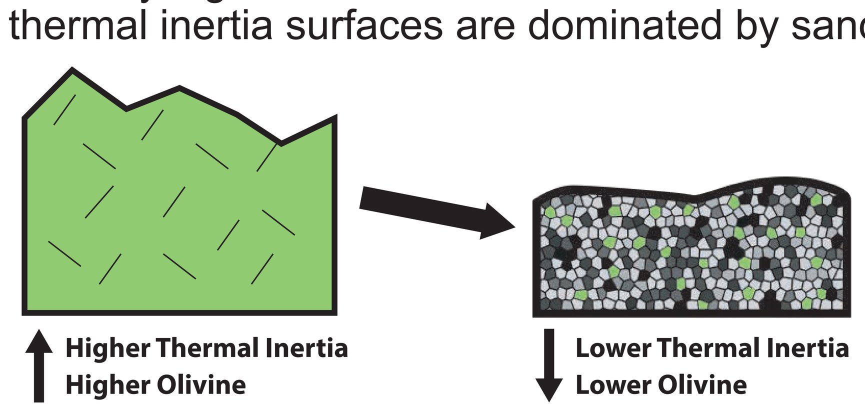


**Figure 1.** Simplified illustration demonstrating weathering of olivine-rich, high inertia bedrock into sediment with lower olivine content and lower thermal inertia.

## OBJECTIVE

We aim to test the hypothesis that chemical weathering has played a dominant role in the production of Martian sediment [11,12] by looking for a positive correlation between olivine content and thermal inertia for several olivine-rich regions on Mars.

## DATA AND METHODS

- For each region data extracted from MGS Thermal Emission Spectrometer (TES)
  - Varied ROIs delineated to investigate correlation dependence on location and size of ROI
  - TES selection criteria: OCKs 1583-8000, incidence 0-90˚, emission 0-10˚, target temp 250-350 K, thermal inertia quality 0-3, dust cover index (DCI) [13] $\geq$ 0.962, water-ice opacity $\leq$ 0.2, dust opacity $\leq$ 0.1
  - Daytime bolometer-derived thermal inertia from TES database [14]
  - Total olivine content via TES spectral analysis [15]
  - Non-zero total olivine plotted against thermal inertia for each region and the linear Pearson correlation coefficient calculated using IDL
  - Square of this coefficient is reported as $R^2$ (values of > ~0.6 indicative of positive correlation)
- THEMIS DCS 875 images used to delineate ROIs and verify olivine signatures [e.g. 16]
- Seasonal variance on TES-derived thermal inertia investigated for each region [17]
  - For largest ROI, extracted 3 years (OCKs 158-24,346) of daytime TES data with thermal inertia quality 0-3, water-ice opacity $\leq$ 0.2, dust opacity $\leq$ 0.1
  - Bolometric thermal inertia binned by 10° $L_s$ and a median thermal inertia calculated for each bin
  - Mean and standard deviation of these bin medians used to determine subset of $L_s$ observations

## 1. NILI FOSSAE

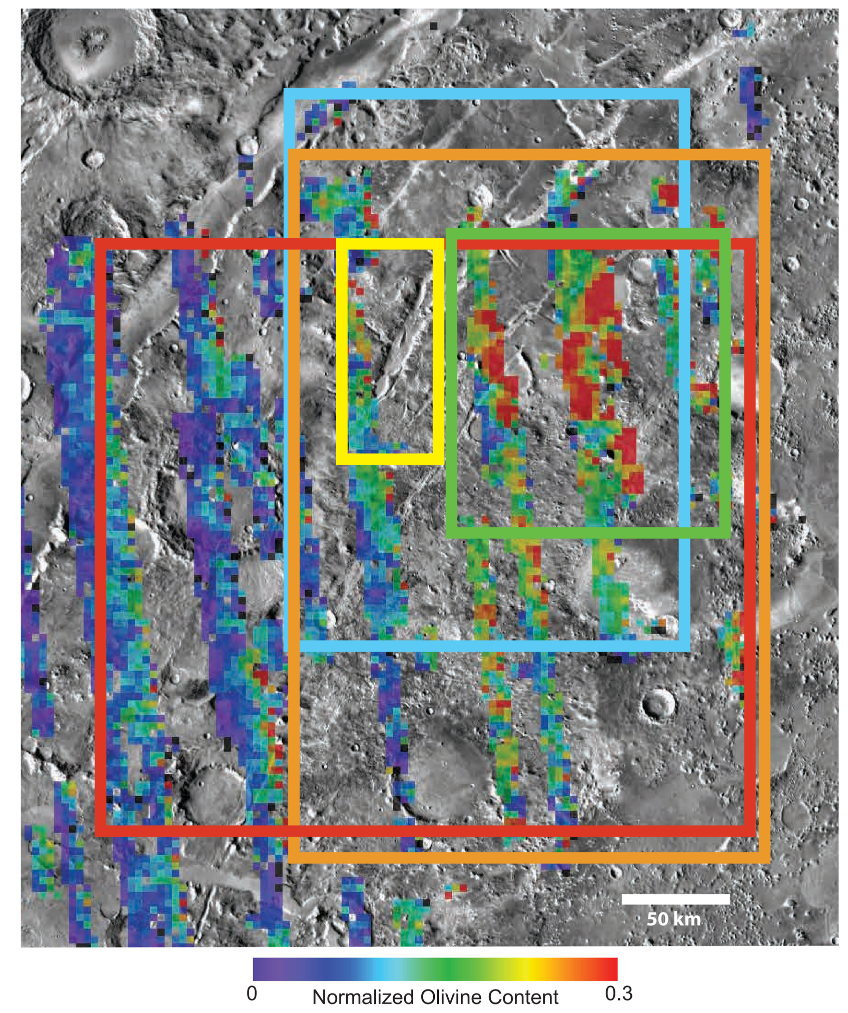


**Figure 2.** Region around the Nili Fossae showing location of ROIs. Image centered at 77.8˚ E, 20.7˚ N. Background greyscale mosaic is 100 m/pixel THEMIS relative daytime temperature [18] overlain with TES footprints colored by total olivine content [15].

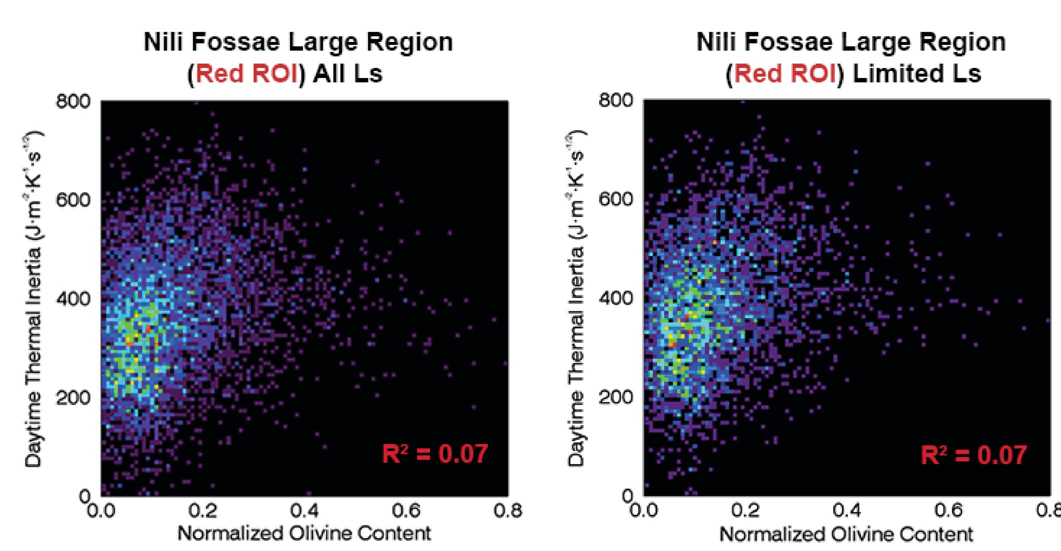


**Figure 3.** Normalized olivine content versus thermal inertia within red ROI (Figure 2). Limiting observations by $L_S$ does not affect correlation.

| ROI | All $L_S$ # non-zero olivine observations | All $L_S$ $R^2$ | Limited $L_S$ # non-zero olivine observations | Limited $L_S$ $R^2$ |
|---|---|---|---|---|
| Red | 5086 | 0.07 | 3640 | 0.07 |
| Orange | 3576 | 0.01 | 2551 | 0.01 |
| Cyan | 2819 | 0.03 | 2098 | 0.03 |
| Green | 1332 | 0.00 | 1005 | 0.01 |
| Yellow | 286 | 0.02 | 277 | 0.02 |

**Table 1.** ROI colors designated correspond to Figure 2.

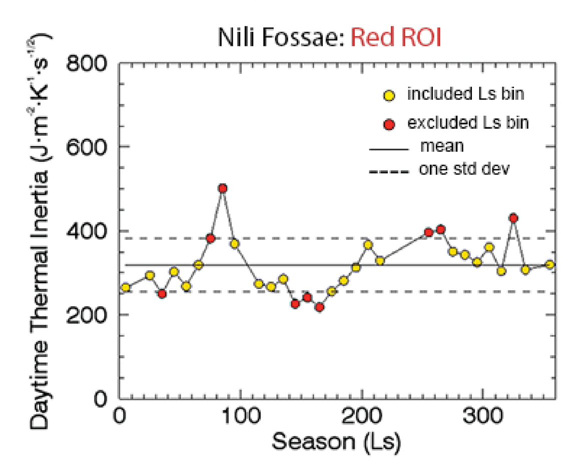


**Figure 4.** Median thermal inertia for each 10° $L_S$ bin used to determine limited $L_S$ for correlation analysis (Table 1).

## 2. AURORAE PLANUM

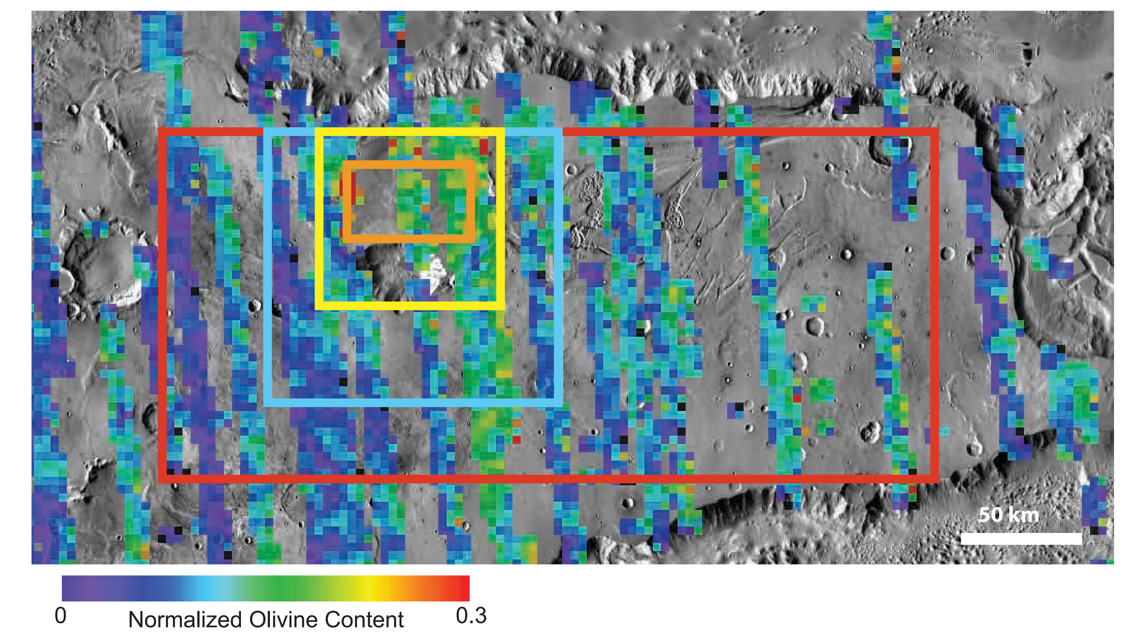


**Figure 5.** Location of ROIs in Aurorae Planum. Image centered at 309.7˚ E, 10.3˚ S. Background greyscale mosaic is 100 m/pixel THEMIS relative daytime temperature [18] overlain with TES footprints colored by total olivine content [15].

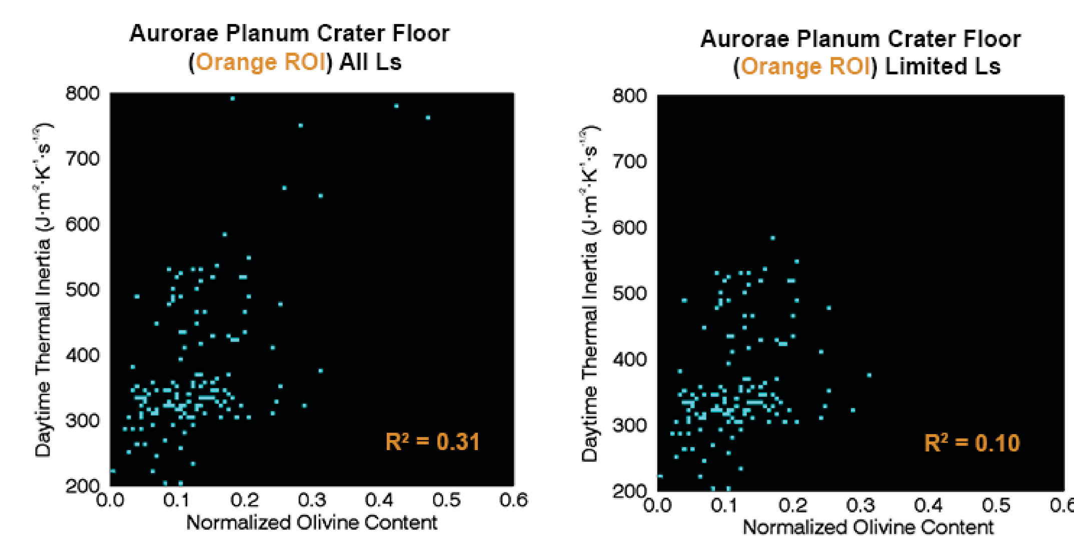


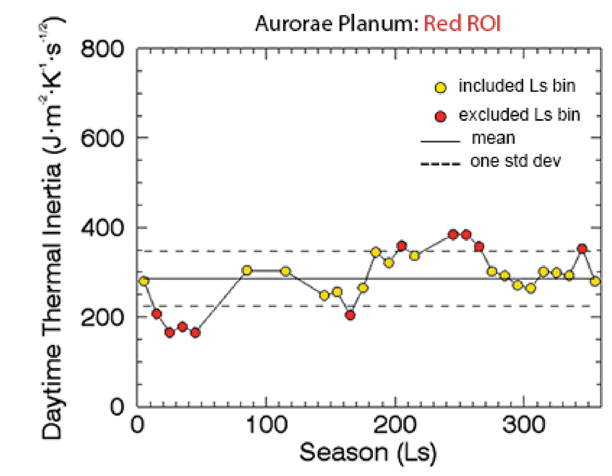


**Figure 6.** Median thermal inertia for each 10° $L_S$ bin used to determine limited $L_S$ for correlation analysis (Table 2).

| ROI | All $L_S$ # non-zero olivine observations | All $L_S$ $R^2$ | Limited $L_S$ # non-zero olivine observations | Limited $L_S$ $R^2$ |
|---|---|---|---|---|
| Red | 4047 | 0.01 | 3124 | 0.01 |
| Cyan | 1384 | 0.02 | 1142 | 0.02 |
| Yellow | 496 | 0.06 | 430 | 0.05 |
| Orange | 145 | 0.31 | 138 | 0.10 |

**Table 2.** ROI colors designated correspond to Figure 5.

**Figure 7.** Normalized olivine content versus thermal inertia for observations within orange ROI on crater floor. Limiting observations by Ls eliminates 7 data points and significantly decreases correlation.

## 3. SOUTH ISIDIS

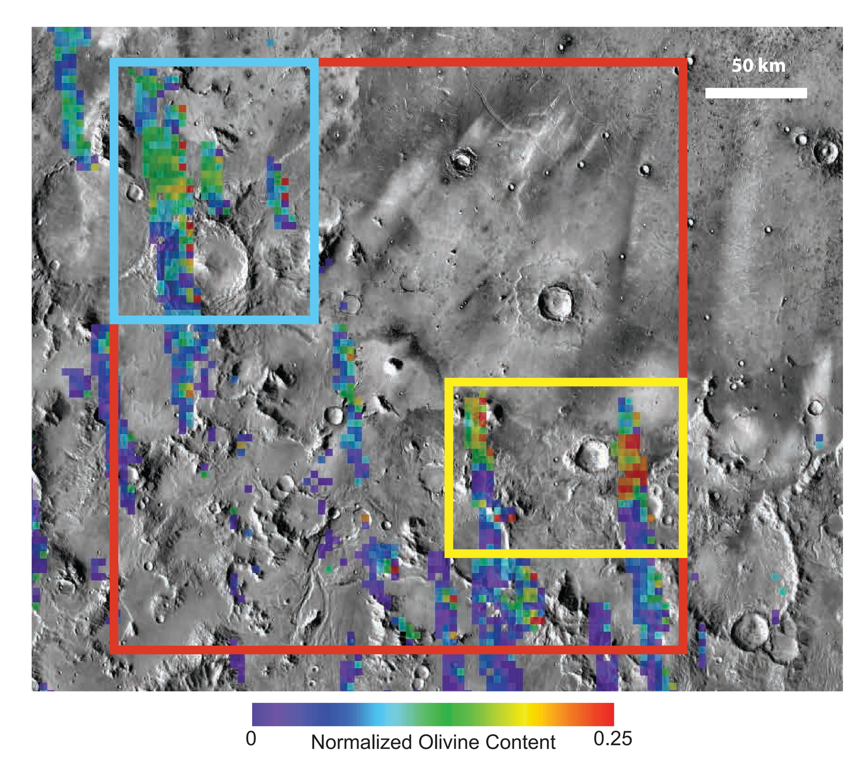


**Figure 8.** Location of ROIs in South Isidis. Image centered at 83.0 E, 4.5˚ N. Background greyscale mosaic is 100 m/pixel THEMIS relative daytime temperature [18] overlain with TES footprints colored by total olivine content [15].

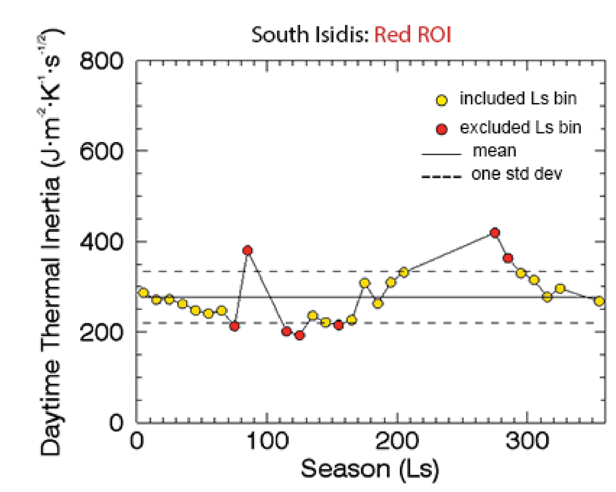


**Figure 9.** Median thermal inertia for each 10° $L_S$ bin used to determine limited $L_S$ for correlation analysis (Table 3).

| ROI | All $L_S$ # non-zero olivine observations | All $L_S$ $R^2$ | Limited $L_S$ # non-zero olivine observations | Limited $L_S$ $R^2$ |
|---|---|---|---|---|
| Red | 825 | 0.04 | 615 | 0.02 |
| Yellow | 188 | 0.01 | 127 | 0.03 |
| Cyan | 171 | 0.10 | 84 | 0.10 |

**Table 3.** ROI colors designated correspond to Figure 8.

## OBSERVATIONS

- **For all regions and all ROIs, no correlation between non-zero olivine content and thermal inertia was found.**
- Size and location of ROI within region influenced calculated $R^2$
  - In Nili Fossae, largest $R^2$ (0.07) found when including western region dominated by lower olivine contents
  - Apparent increase in correlation only significant if westward deposits are genetically related to higher olivine materials to the east
  - In Aurorae Planum, largest $R^2$ (0.31) found when limiting ROI to crater floor (orange ROI)
  - → ***Understanding of local geology is important when defining ROIs and interpreting results***
- Limiting by $L_s$ influenced calculated $R^2$ in some ROIs
  - Most significant in Aurorae Planum for crater floor (orange) ROI; $R^2$ decreased from 0.3 to 0.1
  - Limiting by $L_s$ could influence results if olivine content and thermal inertia are positively correlated (or nearly so)
- [12] found a non-perfect but positive qualitative correlation between olivine content and thermal inertia around the Nili Fossae
  - We find no correlation using TES data, quantitatively exposing this non-perfect correlation
  - OMEGA and CRISM show phyllosilicate-bearing and (olivine-poor) mafic units exposed around the Nili Fossae at scales much smaller than individual TES footprint [19]
  - → ***Assumption that all lower inertia materials within ROI are derived from higher inertia, olivine-rich materials is invalid***
  - → ***Complicated geological relationships, likely at scales below TES resolution, play a large role in non-correlation between olivine content and thermal inertia***

## ONGOING WORK

- Additional olivine-rich regions (Eos and Ganges Chasmata, Hellas and Argyre Planitia, and Ares Valles) will be examined
- Localized analyses at THEMIS scale will be done so knowledge of local geology can be incorporated with more confidence.

## REFERENCES

[1] Edwards, C.S. et al. (2009) *JGR*, 114, E11001.
[2] Bandfield, J.L. et al. (2000) *Science*, 287, 1626-1630.
[3] Rogers, A.D. and Christensen, P.R. (2007), *JGR*, 112, E01003.
[4] Bibring, J.-P. et al. (2005) *Science*, 307, 1576-1581.
[5] Mustard, J.F. et al. (2008), *Nature*, 454(7202) 7305-7309.
[6] Milliken, R.E. et al. (2008), *Geology*, 36(11) 847-850.
[7] Squyres, S.W. et al. (2008), *Science*, 320, 5879, 1063-1067.
[8] Tosca, N.J. et al. (2004) *JGR*, 109, E05003.
[9] Stopar, J.D. et al. (2006) *GCA*, 70(24), 6136-6152.
[10] Hurowitz, J.A. et al. (2006) *JGR*, 111, E02S19.
[11] Bandfield, J.L. et al. (2008) *Geology*, 36(7), 579-582.
[12] Bandfield, J.L. et al. (2011), *Icarus*, 211, 157-171.
[13] Ruff, S.W. et al. (2002), *JGR*, 107, E12, 5127.
[14] Mellon, M.T. et al. (2000) *Icarus*, 148, 437-455.
[15] Koeppen, W.C. and Hamilton, V. E. (2008) *JGR*, 113.
[16] Hamilton, V.E. and Christensen, P.R. (2005) *Geology*, 33, 433-436.
[17] Putzig, N.E. and Mellon, M.T. (2007) *Icarus*, 191, 68-94.
[18] Edwards, C.S. et al. (2011) *JGR*, 116, E10008.
[19] Mustard, J.F. et al. (2009) *JGR*, 114, E00D12.

## ACKNOWLEDGEMENTS

This work was funded by a grant to VEH from the Mars Data Analysis Program (NNX11A183G)